Available online at www.sciencedirect.com
ScienceDirect
Biochimica et Biophysica Acta 1770 (2007) 1151–1160
www.elsevier.com/locate/bbagen

Mutations of Trp275 and Trp397 altered the binding selectivity of *Vibrio carchariae* chitinase A

Wipa Suginta [a,*], Chomphunuch Songsiriritthigul [a,b], Archara Kobdaj [a], Rodjana Opassiri [a], Jisnuson Svasti [c]

[a] *School of Biochemistry, Institute of Science, Suranaree University of Technology, Nakhon Ratchasima 30000, Thailand*
[b] *National Synchrotron Research Center, P.O. Box 93, Nakhon Ratchasima 30000, Thailand*
[c] *The Department of Biochemistry and Center for Protein Structure and Function, Faculty of Science, Mahidol University, Bangkok, Thailand*

Received 7 November 2006; received in revised form 19 March 2007; accepted 22 March 2007
Available online 4 April 2007

Abstract

Point mutations of the active-site residues Trp168, Tyr171, Trp275, Trp397, Trp570 and Asp392 were introduced to *Vibrio carchariae* chitinase A. The modeled 3D structure of the enzyme illustrated that these residues fully occupied the substrate binding cleft and it was found that their mutation greatly reduced the hydrolyzing activity against *p*NP-$[GlcNAc]_2$ and colloidal chitin. Mutant W397F was the only exception, as it instead enhanced the hydrolysis of the *p*NP substrate to 142% and gave no activity loss towards colloidal chitin. The kinetic study with the *p*NP substrate demonstrated that the mutations caused impaired K_m and k_{cat} values of the enzyme. A chitin binding assay showed that mutations of the aromatic residues did not change the binding equilibrium. Product analysis by thin layer chromatography showed higher efficiency of W275G and W397F in G4–G6 hydrolysis over the wild type enzyme. Though the time course of colloidal chitin hydrolysis displayed no difference in the cleavage behavior of the chitinase variants, the time course of G6 hydrolysis exhibited distinct hydrolytic patterns between wild-type and mutants W275G and W397F. Wild type initially hydrolyzed G6 to G4 and G2, and finally G2 was formed as the major end product. W275G primarily created G2–G5 intermediates, and later G2 and G3 were formed as stable products. In contrast, W397F initially produced G1–G5, and then the high-M_r intermediates (G3–G5) were broken down to G1 and G2 end products. This modification of the cleavage patterns of chitooligomers suggested that residues Trp275 and Trp397 are involved in defining the binding selectivity of the enzyme to soluble substrates.
© 2007 Elsevier B.V. All rights reserved.

Keywords: Active-site mutation; Chitin hydrolysis; Chitinase A; Chitooligosaccharide; Specific hydrolyzing activity; Thin layer chromatography; *Vibrio carchariae*

1. Introduction

Chitin is a β (1,4)-linked homopolymer of *N*-acetylglucosamine (GlcNAc or G1) and mainly found as a structural component of fungal cell walls and the exoskeletons of invertebrates, including insects and crustaceans. A complete hydrolysis of chitin usually requires three classes of glycosyl hydrolases. Endochitinases (EC 3.2.1.14) act randomly on chitin to give chitoligomers, then chitobioses ($[GlcNAc]_2$ or G2) as the main products. Chitobiases (EC 3.2.1.52 or formally EC 3.2.1.30) and *N*-acetyl-β-hexosaminidases (EC 3.2.1.52) further hydrolyze the dimers and chitoligomers to yield *N*-acetylglucosamine (GlcNAc or G1) as the final product. Chitinases occur in a wide range of organisms, including viruses, bacteria, fungi, insects, higher plants, and humans. The presence of chitinases in such organisms is closely related to the physiological roles of their substrates. For example, bacteria express chitinases that enable them to utilize chitin biomass as the sole source of carbon and nitrogen [1], whilst chitinases in fungi are thought to have autolytic, nutritional and morphogenetic functions [2]. In insects, chitinases are essential in the moulting process, and may also affect gut physiology through their involvement in peritrophic membrane turnover [3]. Plant chitinases mainly act as biological control agents against fungal

Abbreviations: Gn, β-1–4 linked oligomers of GlcNAc residues where $n=1–6$; *p*NP-$(GlcNAc)_2$, 4-nitrophenyl *N,N'*-diacetyl-β-D-chitobioside; TLC, thin-layer chromatography; DMAB, *p*-dimethylaminobenzaldehyde; IPTG, isopropyl thio-β-D-galactoside; PMSF, phenylmethylsulphonylfluoride

* Corresponding author. Tel.: +66 44 224313; fax: +66 44 224193.
E-mail address: wipa@sut.ac.th (W. Suginta).

0304-4165/$ - see front matter © 2007 Elsevier B.V. All rights reserved.
doi:10.1016/j.bbagen.2007.03.012

pathogens and invading insects [4,5], while viral chitinases are involved in pathogenesis of host cells [6]. Chitinases in some vertebrates are mainly produced as part of their digestive tract and may also utilize the enzymes in their defense against pathogenic fungi and some parasites. Human chitinases are particularly associated with anti-inflammatory effect against the T helper-2 driven diseases, such as allergic asthma [7,8].

Chitin is the second most prominent polymer only after cellulose. Thus, the enzymatic degradation of chitin waste using chitinases has recently received much attention as an environmentally-friendly alternative to chemical methods. Chitin derivatives are highly biocompatible and offer a diverse range of applications in areas such as biomedicine, nutrition, food processing, and cosmetics. Chitinase A is a major chitinase produced at high levels by certain soil-born and marine bacteria. This enzyme could potentially serve as an efficient catalyst for the bioconversion of chitin into valuable derivatives for commercial use.

We previously reported the isolation of chitinase A from a Gram-negative marine bacterium, *Vibrio carchariae*, and the DNA that encodes the *Chi A* gene [9,10]. On the basis of amino acid sequence similarities, this M_r 63000 enzyme is classified as a member of family 18 chitinases [11]. Like other family-18 microbial enzymes [12–14], the catalytic domain of *V. carchariae* enzyme comprises two short sequence regions, which form an $(\alpha/\beta)_8$-TIM barrel active site. A completely conserved acidic amino acid (Glu315) located at the end of the conserved motif DxxDxDxE (in the β4 strand) is likely to be the catalytic residue [10]. The action of native chitinase A on chitin initially released a series of small chitooligomeric fragments, which were further hydrolyzed to G2 as the end product, suggesting that the enzyme acts as an endochitinase [15]. The retention of the β over α anomer of all the products observed at initial time of the reactions is in agreement with the substrate-assisted mechanism employed by the enzyme. As suggested by molecular simulation and X-ray structures of the family 18 glycosyl hydrolases [16–19], the catalytic acid equivalent to Glu315 is presumed to donate a proton to the glycosidic oxygen, which leads to a distortion of the sugar molecule at the scissile position into a boat conformation. The resultant bond cleavage yields an oxazolinium intermediate and the retention of anomeric configuration in the products. The higher affinity of *V. carchariae* chitinase A for higher M_r chitooligosaccharides [15] suggested that the catalytic cleft of the enzyme comprises an array of most probably six binding subsites, comparable to that of CiX1 from *Coccidioides immitis* [20,21] and chitinase A (*Sm*chiA) from *Serratia marcescens* [12,22].

A number of studies using site-directed mutagenesis of *Bacillus circulans* chitinase A1, *S. marcescens* 2170 chitinase A and B, and *Streptomyces griseus* chitinase C [23–26] suggested several surface exposed aromatic residues that were important for guiding the chitin chain to the catalytic cleft so that effective catalysis can take place. The effects of the active-site aromatic residues of *B. circulans* chitinase A1 on chitin hydrolysis were also well studied by Watanabe's group [27]. Since the amino acid alignment indicated that certain aromatic residues of *V. carchariae* chitinase A including Tyr171, Trp168, Trp275, Trp397 and Trp570 are linearly aligned with the aromatic residues at the binding cleft of *B. circulans* chitinase A1 and of *S. marcescens* chitinase A, this research has employed site-directed mutagenesis to investigate the roles of these aromatic residues on the binding and hydrolytic activities of the enzyme towards insoluble chitin and soluble chitooligosaccharides.

2. Materials and methods

2.1. Bacterial strains and chemicals

Escherichia coli type strain DH5α was used for routine cloning, subcloning and plasmid preparation. Supercompetent *E. coli* XL1Blue (Stratagene, La Jolla, CA, USA) was the host strain for the production of mutagenized DNA. *E. coli* type strain M15 (Qiagen, Valencia, CA, USA) and the pQE 60 expression vector harboring *chitinase A* gene fragments were used for a high-level expression of recombinant chitinases. Chitooligosaccharides (G1–G6) and *p*NP-glycosides were obtained from Seikagaku Corporation (Bioactive Co., Ltd., Bangkok, Thailand). Flake chitin from crab shells was product of Sigma-Aldrich Pte Ltd., The Capricorn, Singapore Science Park II, Singapore). QuickChange Site-Directed Mutagenesis Kit including *P*fu Turbo DNA polymerase was purchased from Stratagene. Aluminum sheets (Silica gel $60F_{254}$, 20 × 20 cm) for thin-layer chromatography (TLC) were obtained from Merck Co. (Berlin, Germany). Restriction enzymes and DNA modifying enzymes were products of New England Biolabs, Inc. (Beverly, MA, USA). All other chemicals and reagents (analytical grade) were obtained from the following sources: reagents for bacterial media (Scharlau Chemie S.A., Barcelona, Spain.); chitin from crab shells and all chemicals for protein preparation and thin-layer chromatography (Sigma-Aldrich Pte Ltd., Singapore and Carlo Erba Reagenti SpA, Limito, Italy).

2.2. Homology modeling

The putative amino acid sequence of the mature *V. carchariae* chitinase A was submitted to Swiss-Model (http://swissmodel.expasy.org/) for the tertiary structure prediction using the X-ray structure of *S. marcescens* chi A E315L mutant complex with hexaNAG (G6) (PDB code: 1NH6) as structural template. The predicted structure was viewed and edited with Pymol (www.pymol.org). The residues at the substrate binding cleft of *V. carchariae* chitinase A were located by superimposing 459 residues of *V. carchariae* chitinase A with the equivalent residues of *S. marcescens* chi A mutant docked with G6 coordinates, using the program Superpose available in the CCP4 suit [28].

2.3. Mutant design and site-directed mutagenesis

Point mutations were introduced to the wild-type *chitinase A* DNA that was previously cloned into the pQE expression vector by PCR technique [10], using the QuickChange Site-Directed Mutagenesis Kit, according to the Manufacturer's protocols. Active-site chitinase A variants were generated using oligonucleotides synthesized from Proligo Pte Ltd. (Helios, Singapore) and Bio Service Unit (BSU) (Bangkok, Thailand). Oligonucleotide sequences used for site-directed mutagenesis are listed in Table 1. Single mutants (W168G, Y171G, W275G, W397F, W570G and D392N) were constructed using the DNA fragment encoding wild-type chitinase A as template. A double mutant (W397F/W570G), a triple mutant (W397F/W570G/ W275G), and a quadruple mutant (W397F/W570G/W275G/Y171G) were produced using mutants W570G, W397F/W570G, and W397F/W570G/W275G, respectively, as DNA templates.

The success of newly-generated mutations was confirmed by automated DNA sequencing (BSU, Thailand). The programs used for nucleotide sequence analyses were obtained from the DNASTAR package (DNASTAR, Inc., Madison, USA).

2.4. Protein expression and purification

The DNA fragment that encodes wild-type chitinase A (amino acid residues 22–597, without the 598–850 *C*-terminal fragment) was cloned into

Table 1
Primers used for mutagenesis

Name	DNA template	Sequence[a]
W168G	*Chitinase A* wild-type	forward 5′-CTTATTTTGTTGAAGGAGGCATCTACGG-3′ reverse 5′-CCGTAGATGCCTCCTTCAACAAAATAAG-3′
Y171G	*Chitinase A* wild-type	forward 5′-GAATGGGGCATCGGAGGTCGTGATTACAC-3′ reverse 5′-GTGTAATCACGACCTCCGATGCCCCATTC-3′
W275G	*Chitinase A* wild-type	forward 5′-CATCTATCGGTGGTGGAACAC TTT CTGAC-3′ reverse 5′-GTCAGAAAGTGTTCCACCACCGATAGATG-3′
D392N	*Chitinase A* wild-type	forward 5′-CTTTGCGATGACTTACAACTTCTACGGCGG-3′ reverse 5′-CAGCCGCCGTAGAAGTTGTAAGTCATCGCAAAG-3′
W397F	*Chitinase A* wild-type	forward 5′-GACTTCTACGGCGGCTTCAACAACGTTCC-3′ reverse 5′-GGAACGTTGTTGAAGCCGCCGTAGAAGTC-3′
W570G	*Chitinase A* wild-type	forward 5′-GCAGGTCTATTCTCTGGAGAGATTGATGC-3′ reverse 5′-GCATCAATCTCTCCAGAGAATAGACCTGC-3′
Double mutant	W570G mutant	forward 5′-GACTTCTACGGCGGCTTCAACAACGTTCC-3′ reverse 5′-GGAACGTTGTTGAAGCCGCCGTAGAAGTC-3′
Triple mutant	double mutant	forward 5′-CATCTATCGGTGGTGGAACAC TTT CTGAC-3′ reverse 5′-GTCAGAAAGTGTTCCACCACCGATAGATG-3′
Quadruple mutant	triple mutant	forward 5′-GAATGGGGCATCGGAGGTCGTGATTACAC-3′ reverse 5′-GTGTAATCACGACCTCCGATGCCCCATTC-3′

[a] Sequences underlined indicate mutated codons.

the pQE60 expression vector and highly expressed in *E. coli* M15 cells as the 576-amino acid fragment with a *C*-terminal $(His)_6$ sequence [10]. For recombinant expression, the cells were grown at 37 °C in Luria Bertani (LB) medium containing 100 μg/ml ampicillin until OD_{600} of the cell culture reached 0.6. After that, the cell culture was cooled down on ice to 25 °C before chitinase expression was induced by the addition of isopropyl thio-β-D-galactoside (IPTG) to a final concentration of 0.5 mM. Cell growth was continued at 25 °C for 18 h, and the cell pellet was collected by centrifugation at 4500×*g* for 30 min. The freshly-prepared cell pellet was resuspended in 40 ml of lysis buffer (20 mM Tris–HCl buffer, pH 8.0, containing 150 mM NaCl, 1 mM phenylmethylsulphonyl fluoride (PMSF), and 1.0 mg/ml lysozyme), then lysed on ice using a Sonopuls Ultrasonic homogenizer with a 6-mm-diameter probe (50% duty cycle; amplitude setting, 20%; total time, 30 s, 6–8 times). Unbroken cells and cell debris were removed by centrifugation at 12,000×*g* for 1 h. The supernatant was immediately applied to a Ni-NTA agarose affinity column (1.0×10.0 cm) (QIAGEN GmbH, Hilden, Germany), and the chromatography was carried out gravitationally at 25 °C, following the Qiagen's protocol. After loading, the column was washed with 100 ml of loading buffer (20 mM Tris–HCl buffer, pH 8.0) containing 5 mM imidazole, followed by another 50 ml of 10 mM imidazole in the loading buffer. Ni-NTA-bound proteins were then eluted with 250 mM imidazole in the same buffer. Eluted fractions of 0.5 ml were collected and 6 μl of each fraction was analyzed on a 12% SDS-PAGE, according to the method of Laemmli [29], to confirm purity. Fractions that possessed chitinase activity were pooled and then subjected to several rounds of membrane centrifugation using Vivaspin-20 ultrafiltration membrane concentrators (M_r 10,000 cut-off, Vivascience AG, Hannover, Germany) for a complete removal of imidazole. A final concentration of the protein was determined by Bradford's method [30] using a standard calibration curve constructed from BSA (0–25 μg). The freshly-prepared proteins were either immediately subjected to functional characterization or stored at −30 °C in the presence of 15% glycerol until used.

2.5. Chitinase activity assays

Chitinase activity was determined by colorimetric assay using *p*NP-$[GlcNAc]_2$ as substrate or by reducing sugar assay using colloidal chitin as substrate. The *p*NP assay was determined in a 96-well microtiter plate and a 100-μl assay mixture contained protein sample (10 μl), 500 μM *p*NP-$(GlcNAc)_2$ (25 μl), and 100 mM sodium acetate buffer, pH 5.0 (65 μl). The reaction mixture was incubated at 37 °C for 10 min with constant agitation, then the enzymatic reaction was terminated by the addition of 50 μl 1.0 M Na_2CO_3. The amount of *p*-nitrophenol (*p*NP) released was determined spectrophotometrically at 405 nm in a microtiter plate reader (Applied Biosystems, Foster City, CA, USA). The molar concentrations of *p*NP were calculated from a calibration curve constructed with varying *p*NP from 0 to 30 nmol.

The reducing sugar assay was carried out by modifying the chitinase microassay protocol developed by Bruce et al. [31]. The reaction mixture (400 μl), containing 20 mg of colloidal chitin (prepared based on Hsu and Lockwood, 1975 [32]) in 0.1 M sodium acetate buffer, pH 5.0 and 80 μg chitinase A, was incubated at 37 °C with shaking in a Thermomixer comfort (Eppendorf AG, Hamburg, Germany). After 60 min, the reaction was terminated by boiling at 100 °C for 5 min, and then centrifuged at 2795×*g* for 5 min to precipitate the remaining chitin. A 150-μl supernatant was transferred to a new tube, to which was added 30 μl of 0.8 M potassium tetraborate, followed by boiling for 3 min. After cooling, 900 μl of a freshly prepared *p*-dimethylaminobenzaldehyde (DMAB) solution was added and then incubated at 37 °C for 20 min. A release of reducing sugars was detected by measuring the absorbance at 585 nm (A_{585}). Specific hydrolyzing activity against colloidal chitin was calculated by converting A_{585} to μmoles of reducing sugars using a standard calibration curve constructed with varying G2 from 0 to 4.0 μmol.

2.6. Circular Dichroism (CD) spectroscopy

The purified chitinases were diluted to 0.40 to 1.40 mg/ml in 20 mM Tris/HCl buffer, pH 8.0. CD spectra over three scans were measured using a Jasco J-715 spectropolarimeter (Japan Spectroscopic Co., Japan) at near UV (190 to 250 nm) regions. CD measurements were performed at 25 °C with a scan speed of 20 nm/min, 2 nm bandwidth, 100 mdeg sensitivity, an average response time of 2 s and an optical path length of 0.2 mm. The baseline buffer for all the proteins was 20 mM Tris/HCl buffer, pH 8.0. The baseline was measured and subtracted from each spectrum before the raw data were transformed to mean residue ellipticity (MRE) using the equation: $[\Theta] = (73.33\ m^{\circ})/([prot]_{mM}\ l_{cm}\ n)$, where $[\Theta]$ is the MRE in deg cm^2 d/mol, n is the number of amino acids in the polypeptide chain, m° is the measured ellipticity, and l is the path length in centimeters. The intensity of JASCO standard CSA (non-hygroscopic ammonium (+)-10-camphorsulfonate) at wavelength 290 nm was about 45 units. Therefore, the conversion factor was calculated to be 3300/CSA intensity at 290 nm or 73.33 using the equation above. The molecular weight of each protein was calculated from number of amino acids×mean residue weight. After noise reduction and concentration adjustment, the measured ellipticity was converted to the molar ellipticity, which was plotted versus wavelength.

2.7. Kinetic measurements

Kinetic studies of chitinase A mutants were performed by colorimetric assay in a microtiter plate reader (Applied Biosystems, USA). The reaction mixture (100 μl), containing 0–500 μM *p*NP-$(GlcNAc)_2$, dissolved in 100 mM sodium acetate buffer, pH 5.0, and dH_2O, was pre-incubated at 37 °C for 10 min. After the enzyme (400 ng) was added, the reaction was continued for additional 10 min at 37 °C and then terminated with 50 μl of 1 M Na_2CO_3. Release of *p*-nitrophenol (*p*NP) was monitored at A_{405}, which was subsequently converted to molar quantities using a calibration curve of *p*NP (0–30 nmol). The kinetic values (K_m, V_{max}, and k_{cat}) were evaluated from three independent sets of data by the nonlinear regression function of the GraphPad Prism software (GraphPad Software Inc., San Diego, CA).

2.8. Chitin binding assay

Chitin binding studies were carried out using flake chitin prepared from crab shells (Sigma-Aldrich Pte Ltd., Singapore). Fine particles of insoluble chitin were suspended in dH_2O to yield 10 mg/ml stock solution (the suspension was continuously stirred with a magnetic stirrer in order to obtain consistent amounts when pipetting). A reaction mixture (2.0 ml), containing 2.5 mg/ml flake chitin and 200 μg/ml chitinase in 100 mM sodium acetate buffer, pH 5.0, was shaken continuously at 4 °C. At different time points (0, 5, 10, 15, 30, 60, 90, 120, and 180 min), a 150-μl aliquot was taken and spun twice in a microcentrifuge at 9660×*g* for 3 min to precipitate the chitin particles. Then the unbound chitinase A remaining in the supernatant was measured spectrophotometrically at 280 nm (A_{280}).

2.9. Product analysis by thin-layer chromatography

Hydrolysis of chitooligosaccharides (G2–G6) by wild-type and mutants D392N, W168G, Y171G, W275G, and W397F was carried out in a 80-μl reaction mixture, containing 0.1 M sodium acetate buffer, pH 5.0, 2.5 mM substrate and 800 ng purified enzyme. The reaction was incubated at 30 °C with shaking for 60 min, and then terminated by boiling for 5 min. For product analysis, each reaction mixture was applied five times (one μl each) to a silica TLC plate (7.0×10.0 cm), and then chromatographed three times (1 h each) in a mobile phase containing n-butanol: methanol: 28% ammonia solution: H_2O (10:8:4:2) (v/v), followed by spraying with aniline-diphenylamine reagent and baking at 180 °C for 3 min [33].

In the time course of G6 hydrolysis by wild-type, W275G and W397F were measured in the same way as described for the hydrolysis of G2–G6, but the reaction was incubated at 30 °C at interval times of 2, 5, 10, 15, 30, 60 min, and 18 h prior to termination. Examination of the time course of chitin hydrolysis by the three chitinase variants was carried out in a 400-μl reaction mixture, containing 0.1 M sodium acetate buffer, pH 5.0, 20 mg colloidal chitin, and 80 μg purified enzyme. The reaction was incubated at 30 °C at the same time intervals as for G6 hydrolysis, and then terminated by boiling for 5 min. Products released from the reactions were subsequently analyzed by TLC using the conditions described above.

3. Results and discussion

3.1. Sequence analysis and homology modeling

A comparison of the deduced amino acid sequence of *V. carchariae* chitinase A with seven other family-18 chitinases suggested that Glu315 and Asp392 are completely conserved (data not shown). However, we previously employed site-directed mutagenesis to demonstrate that only Glu315 was important for catalysis [15]. The alignment also showed that five aromatic residues, including Trp168, Tyr171, Trp275, Tyr435, and Trp570 in the sequence of *V. carchariae* chitinase A are linearly aligned with the equivalent aromatic residues of other bacterial sequences. Trp397 is the only residue for which phenylalanine is replaced in the sequences of *S. marcescens*, *B. cepacia*, and *A. punctata*. In an attempt to locate these amino acids in the structure of *V. carchariae* chitinase A, its 3D-structure was modeled based on the X-ray structure of *S. marcescens* Chi A E315L mutant complexed with G6 (see Materials and methods). The target residues, which extend over the substrate binding cleft at the top of the TIM-barrel domain, are shown in Fig. 1A.

Fig. 1B displays the superimposition of the active site of *V. carchariae* chitinase A on that of *S. marcescens* Chi A E315L mutant. It can be seen that Trp168, Tyr171, Trp231, Trp 275, Tyr435, Trp570, Glu315 and Asp392 of the *Vibrio* enzyme completely overlay Trp167, Tyr170, Phe232, Trp275, Trp539, Glu315 and Asp391, respectively, of the *Serratia* enzyme with an R.M.S. value of 0.032 Å. In contrast, Trp397 overlaid Phe396 residue of the *Serratia* enzyme with the orientation of their hydrophobic faces lying perpendicular to each other.

Since the positions of the binding cleft residues of *V. carcharia* and *S. marcescens* chitinases were nearly identical, most of the conformations of the sugar rings bound in the catalytic cleft of the template's structure are likely to be adopted by the modeled structure. Based on this assumption, Tyr171 is likely to be located at the edge of the binding cleft beyond subsite −4 (the non-reducing end), whereas Trp168, Trp570, and Trp275 should stack against the pyranosyl rings of GlcNAc units at subsites −3, −1, and +1, respectively. Trp397 should be located near the GlcNAc unit at subsite +2 (the reducing end). The presence of Glu315 at the scissile bond between the GlcNAcs at subsites −1 and +1 seems to explain the catalytic role of this residue. Asp392 appears to be further away from the cleavage site, but in close contact with the GlcNAcs at subsites +1 and +2. This supports our previous finding that this residue did not play a direct role in catalysis [15].

3.2. Recombinant expression, purification and secondary structure determination

To investigate the influence of Tyr171, Trp168, Trp275, Trp397, Trp570 on the binding and hydrolytic activities of *V. carchariae* chitinase A, these residues were mutated using PCR-based site-directed mutagenesis. Replacement of Asp392 with Asn was previously described by Suginta et al. [15]. After confirming the genetic modification of the target bases by automatic DNA sequencing, the recombinant proteins were highly expressed in *E. coli* M15 host cells. The six histidine residues tagged at the *C*-terminus allowed the proteins to be readily purified using Ni-NTA agarose affinity chromatography. SDS/PAGE analysis showed that the purified proteins migrated to ~63 kDa (Fig. 2A). This molecular weight corresponded well to that of wild-type. The yields obtained from this expression system were approx. 10–15 mg of highly purified protein per liter of bacterial culture.

Prior to further investigating the effects of point mutations on the binding and hydrolytic activities, the folding states of the *E. coli* expressed chitinase A were examined by means of CD spectroscopy. Fig. 2B shows that the spectra of the mutated

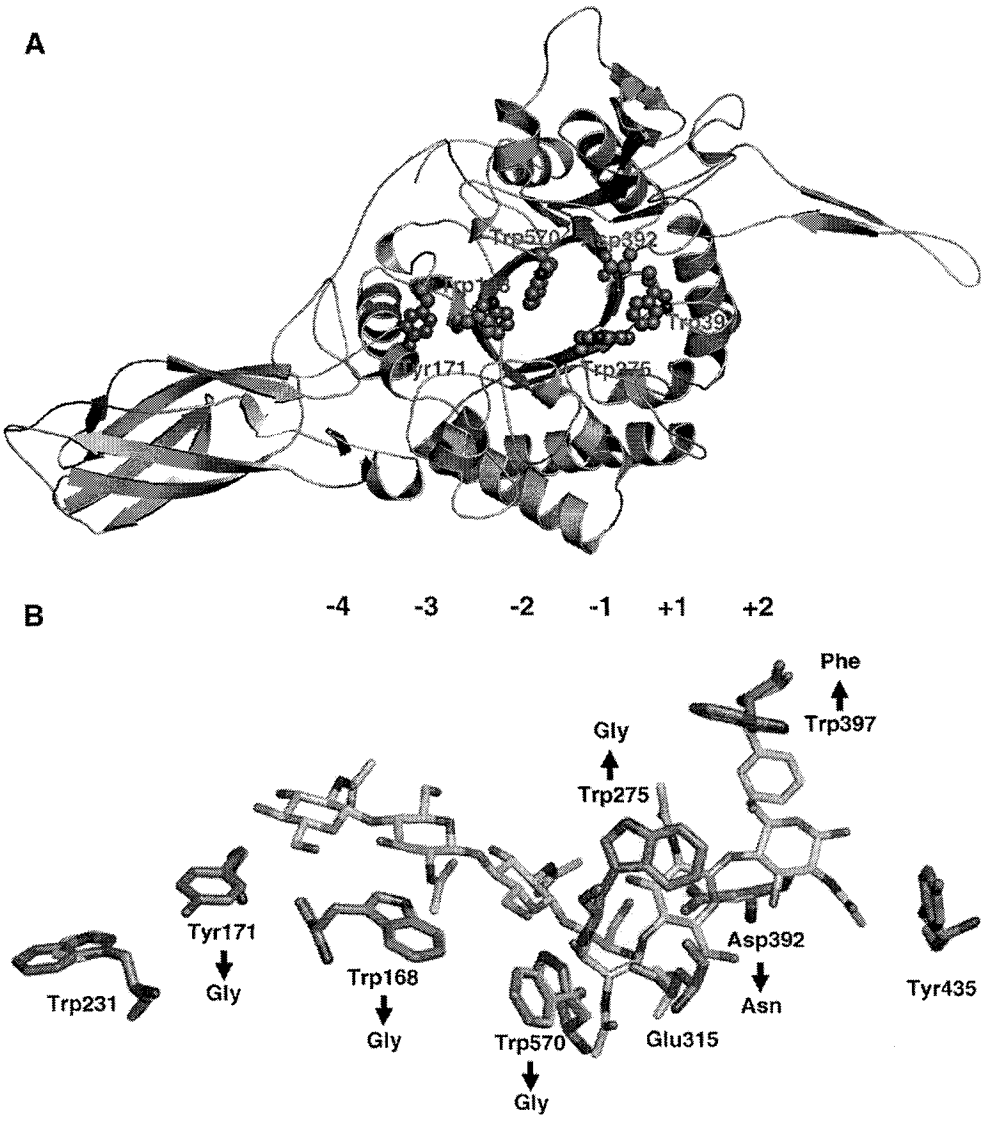

Fig. 1. The Swiss-Model 3D-structure of *V. carchariae* chitinase A. (A) A ribbon representation of the 3D-structure of *V. carchariae* chitinase A (in green) was modeled based on the X-ray structure of *S. marcescens* Chi A E315L mutant as described in the text. The target aromatic residues (in magenta) that line within the substrate-binding cleft are shown in space-filling model. (B) A stick model of the putative binding cleft of *V. carchariae* chitinase A (in magenta) was superimposed on that of *S. marcescens* Chi A E315L mutant (in yellow) complexed with G6 (in cyan). N atoms are shown in blue and O atoms are shown in red.

proteins nicely overlaid the spectrum of the wild-type. This demonstrated the overall similarity of the conformations of mutated and non-mutated enzymes.

3.3. Effects of the mutations on the chitin binding equilibrium and the specific hydrolyzing activity of chitinase A

Initial studies of the chitin binding activity of single mutants were performed using flake chitin prepared from crab shells. To minimize hydrolysis of the enzyme bound to the chitin substrate, the assay mixture was maintained at 4 °C throughout the experiment. For each reaction, a decrease in the concentration of the unbound enzyme was monitored at various time points as indicated in Materials and methods. The results (Fig. 3) showed that the binding behaviors of wild-type enzyme and mutants W168G, Y171G, W275G, and W397F were indistinguishable. In general, the binding process took place quite rapidly, and reached equilibrium within 15 min. However, a difference was seen with mutant D392N for which the binding took a much longer time, about 60 min, to reach equilibrium. Apparently, mutations of the aromatic side chains did not markedly affect the binding equilibrium.

When the specific hydrolyzing activity of the different chitinase variants towards *p*NP-$[GlcNAc]_2$ and colloidal chitin were examined (Table 2), similar results were seen

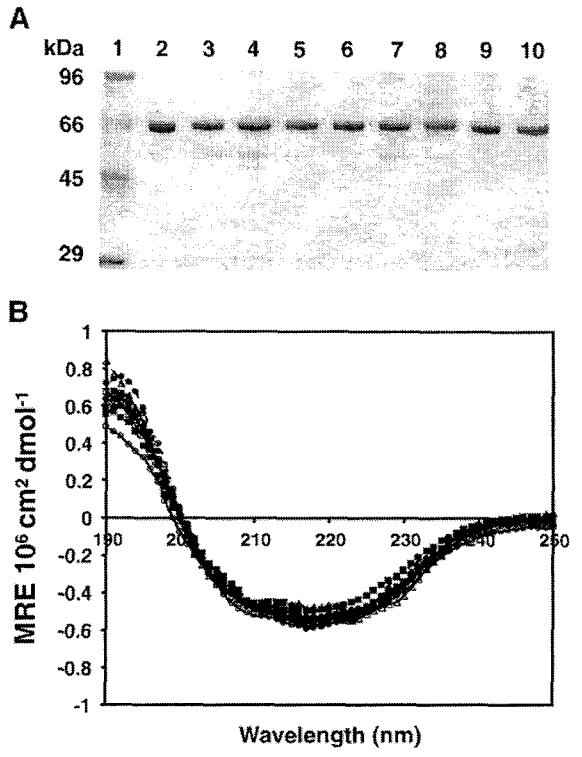

Fig. 2. SDS / PAGE analysis and CD spectra of chitinase A variants. (A) Purified chitinases (2 μg) were electrophoresed using 12% SDS/PAGE gel and then were stained with Coomassie blue. (B) Chitinase A and its mutants were purified by Ni-NTA agarose affinity chromatography, and then dialyzed extensively to remove imidazole. The proteins were solubilized in 20 mM Tris/HCl buffer, pH 8.0 to final concentrations of 0.40 to 1.40 mg/ml. CD spectra of chitinase variants were obtained with a Jasco J-715 spectropolarimeter. A solution of 20 mM Tris/HCl, pH 8.0 was used for background subtraction. Symbols: —○—, wild-type; —□—, D392N; —△—, W168G; —●—, Y171G, —■—, W275G; —▲—, W397F; ---○---, W570G; ---□---, double mutant; ---△---, triple mutant; and ---●---, quadruple mutant.

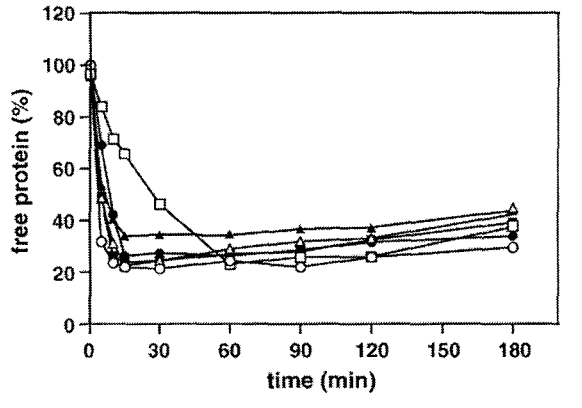

Fig. 3. Time-course studies of binding of chitinase A and mutant enzymes to colliodal chitin. Chitinases (200 μg/ml in 100 mM sodium acetate buffer, pH 5.0) were incubated with 2.5 mg/ml flake chitin at 4 °C to minimize chitin hydrolysis. Decreases in free enzyme concentration were monitored at different time points from 0 to 180 min by measuring A_{280}. Each data value was calculated from triplicate experiments. Symbols: ○, wild-type; □, D392N; △, W168G; ●, Y171G, ■, W275G; and ▲, W397F.

Table 2
Specific hydrolyzing activity of chitinase A and mutants against *p*NP-$[GlcNAc]_2$ and colloidal chitin

Chitinase A variant	Specific hydrolyzing activity	
	($\times 10^{-3}$ μmol *p*NP/min/μg)[a]	(μmol reducing sugars/min/μg)[b]
Wild-type	1.84±0.05 (100)[c]	1.99±0.018 (100)
D392N	0.61±0.09 (33.4)	n.d.[d]
W168G	0.24±0.03 (13.0)	n.d
Y171G	0.36±0.00 (19.5)	n.d.
W275G	0.20±0.00 (11.1)	0.10±0.001 (5.0)
W397F	2.61±0.08 (141.8)	2.04±0.061 (102.5)
W570G	0.11±0.00 (5.6)	n.d.
Double mutant (W570G/W397F)	0.10±0.002 (5.5)	n.d.
Triple mutant (W570G/W397F/W275G)	0.01±0.001 (0.6)	n.d.
Quadruple mutant (W570G/W397F/W275G/Y171G)	0.01±0.001 (0.6)	n.d.

For colorimetric assay A 100-μl assay mixture, containing 400 ng chitinase, 500 μM *p*NP-$(GlcNAc)_2$, and 0.1 M sodium acetate buffer, pH 5.0, was incubated at 37 °C for 10 min, and then terminated by the addition of 50 μl of 1.0 M Na_2CO_3. The amount of *p*NP released was determined by A_{405}. The μmole amount of *p*NP was calculated from a calibration curve of *p*NP (0–30 nmol). With the reducing sugar assay, the reaction mixture (400 μl), containing 20 mg of colloidal chitin, 0.1 M sodium acetate buffer, pH 5.0 and 80 μg chitinase A, was incubated at 37 °C with continuous shaking. After 60 min, the reaction was boiled at 100 °C for 5 min, and then centrifuged to remove the insoluble chitin. Release of reducing sugars was determined according to DMAB method as described in Materials and methods. The μmol amounts of the reducing sugars were estimated using a standard calibration curve of G2 (0–4.0 μmol).

[a] Chitinase activity was measured using *p*NP-$[GlcNAc]_2$, and release of *p*NP was detected by the colorimetric method.

[b] Chitinase activity was measured using colloidal chitin, and release of reducing sugars was detected by the DMAB method.

[c] Values in brackets represent relative activity compared to that of wild-type (set as 100).

[d] n.d. represents no detectable activity.

with both substrates. Mutations of Trp168, Tyr171, Trp570, and D392N completely abolished the hydrolyzing activity against colloidal chitin, and greatly reduced the hydrolyzing activity against the *p*NP substrate. As previously seen with *B. circulans* ChiA1, mutations of the equivalent aromatic residues (Trp53, Tyr56, and Trp433, respectively) to alanine also resulted in a drastic decrease in the hydrolyzing activity of *B. circulans* ChiA1, especially against crystalline β-chitin or colloidal chitin [27]. As proposed by Watanabe [23,27,34], Trp53 and Tyr56 (the equivalent residues of Trp168 and Tyr171 of the *Vibrio* chitinase) participate in the feeding process that brings the incoming chitin chain through the binding cleft.

At this point, it is difficult to draw a conclusion why mutations of Trp168 and Tyr171 also affected the hydrolyzing activity against the *p*NP substrate, as the $[GlcNAc]_2$ moieties could only bind to subsites −2 and −1 to allow the *p*NP aglycone to bind at subsite +1 for further cleavage.

Of all single mutants, W570G showed most severe effects on the hydrolyzing activity, having no activity against colloidal chitin and least activity (5% remaining activity) against *p*NP-$[GlcNAc]_2$. In the modeled 3D structure (see

Table 3
Kinetic parameters of wild-type and mutants of chitinase A

Chitinase A variants	K_m [a] (μM)	V_{max} (nmol/min/μg chitinase)	k_{cat} (s^{-1})	k_{cat}/K_m (s^{-1} M^{-1})
Wild-type	288±26.0	1.94±0.09	2.15	7.16×10^2 (100)[b]
D392N	71±5.5	0.29±0.01	0.31	4.34×10^2 (61)
W168G	278±28.2	0.10±0.01	0.11	3.82×10^1 (5)
Y171G	115±10.2	0.20±0.001	0.21	1.85×10^2 (26)
W275G	62±10.8	0.11±0.001	0.12	1.89×10^2 (26)
W397F	315±26.7	2.44±0.11	2.59	8.23×10^2 (114)

The hydrolysis of *p*NP-[GlcNAc]$_2$ at varying concentrations of 0–500 μM was carried out with 400 ng native chitnase A in 100 mM sodium acetate buffer, pH 5.0 for 10 min at 30 °C, and then the reaction was terminated with 50 μl of 1 M Na_2CO_3. Release of *p*NP, monitored at A_{405}, was converted to molar quantities using a calibration curve of *p*NP (0–30 nmol). The kinetic values (K_m, V_{max}, and k_{cat}) were determined by nonlinear regression using GraphPad Prism software (GraphPad Software Inc., San Diego, CA).

[a] Kinetic assays were preformed with *p*NP-[GlcNAc]$_2$ as described in Materials and methods. Results are average of three independent experiments.

[b] Numbers in brackets reveal relative k_{cat}/K_m values of the generated mutants by comparing with the wild-type value (set to 100).

Fig. 1B), Trp570 was closest to the sugar ring at subsite-1. Like Trp539 in the *Serratia* structure [22], this residue is likely to be responsible for holding the GlcNAc ring at this position in place so that cleavage of the glycosidic bond between subsites −1 and +1 can occur.

Trp397 was an exception. Its mutation to Phe, instead, enhanced hydrolyzing activity towards the *p*NP substrate to 142% but increased the activity towards colloidal chitin only slightly to 102.5%. Although the elevated activity against *p*NP-[GlcNAc]$_2$ cannot be explained at this stage, the lack of change in the hydrolyzing activity towards the chitin polymer implied that Trp397 did not participate directly in the hydrolytic process.

In addition, the triple and quadruple mutants yielded non-detectable activity against colloidal chitin and less than 1% remaining activity against *p*NP-[GlcNAc]$_2$. This may be seen as the cumulative effects of multiple point mutations on the hydrolyzing activity of *Vibrio* chitinase A.

3.4. Steady-state kinetics of chitinase A variants against *pNP-[GlcNAc]$_2$*

The kinetic parameters of the hydrolytic activity of wild-type and its single mutants (except for W570G) were further explored with *p*NP-[GlcNAc]$_2$. As shown in Table 3, the active-site modifications resulted in impairment of both K_m and k_{cat} of the enzyme. Mutants D392N, Y171G and W275G particularly reduced the K_m values to 0.24, 0.4 and 0.2 times, respectively, of the wild-type's value, while mutant W168G did not significantly change the K_m value against the *p*NP substrate. It is visible that the same mutants also greatly reduced the k_{cat} values to 5–14% of that of the wild-type. Overall, the mutations varied the k_{cat}/K_m values of the enzyme. W168G displayed the least value (5%), followed by Y171G and W275G (approx. 26%), and D392N (61%), compared to the value obtained for wild-type.

On the other hand, mutant W397F gave no significant changes in the kinetic parameters of the enzyme with *p*NP-[GlcNA]$_2$. Its K_m and k_{cat} values were found to be 1.1 and 1.2 fold of that of the wild-type. These data suggested that Trp397 did not take part in the hydrolysis of this substrate.

3.5. TLC analysis of the hydrolytic activity of chitinase variants

The effects of the mutations on the hydrolytic activities against chitooligomers (G2–G6) and colloidal chitin were further studied by thin layer chromatography (TLC). The cleavage patterns of each mutant were initially observed at a single point in time (60 min). As expected, none of the mutants hydrolyzed G2 substrate, as it only acts as the end product of the enzyme action [15]. With G3 substrate (Fig. 4A), W397F was the only mutant that degraded G3 to G1 and G2, while the wild-type and other mutants did not utilize G3 at all. Our recent study showed high K_m value (10.54 mM) of the native enzyme towards G3, indicating that G3 was a poor substrate for *V. carchariae* chitinase [15].

Distinct patterns of product formation became visible with longer-chain oligomers (G4–G6). With G4 substrate (Fig. 4B), the formation of G2 was seen at higher levels with mutants

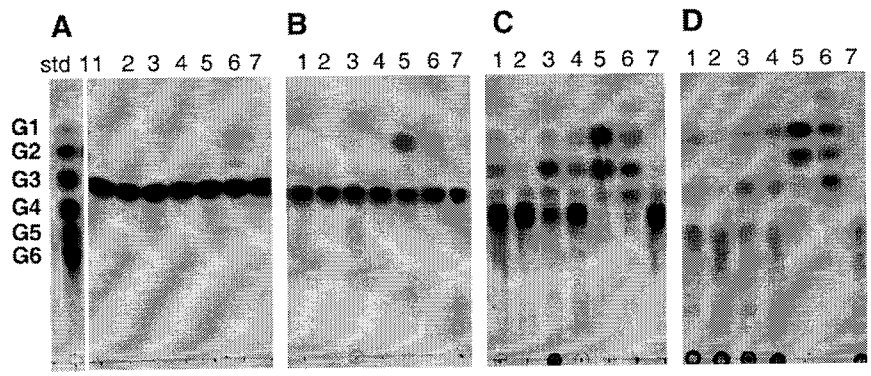

Fig. 4. TLC analysis of chitooligosaccharide hydrolysis of chitinase A and mutants. A reaction mixture, containing 400 ng chitinase and 2.5 mM substrate (G2–G6) in 100 mM sodium acetate buffer, pH 5.0, was incubated for 60 min at 30 °C. After boiling, the reaction solution (5 μl) was analyzed on TLC and sugar products detected with aniline-diphenylamine reagent. (A) Hydrolysis of G3 substrate, (B) Hydrolysis of G4 substrate, (C) Hydrolysis of G5 substrate, and (D) Hydrolysis of G6 substrate. Lanes: std, standard mix of G1–G6; 1, wild-type; 2, D392N; 3, W168G; 4, Y171G, 5, W275G; 6, W397F; and 7, substrate control.

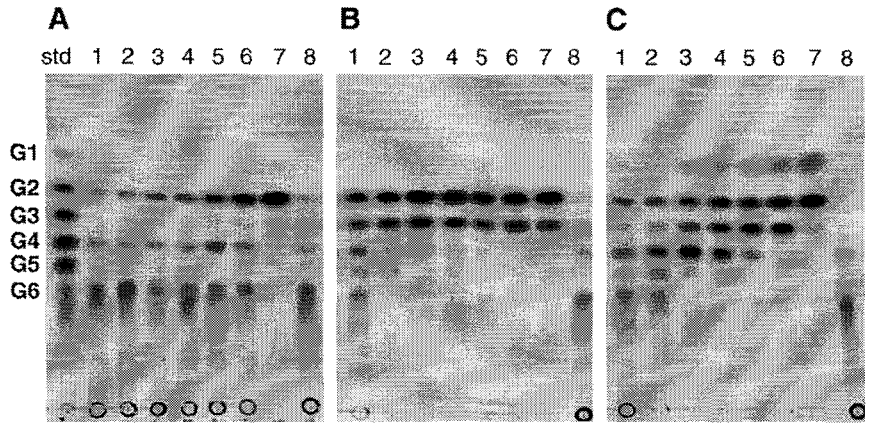

Fig. 5. Time-course of G6 hydrolysis by wild-type and mutants W275G and W397F. A reaction mixture (80 μl), containing 800 ng wild-type (A), W275G (B), or W397F (C) and 2.5 mM G6 in 0.1 M sodium acetate buffer, pH 5.0, was incubated at various times at 30 °C, and then analyzed by TLC. Sugar products were detected with aniline-diphenylamine reagent. Lanes: std, a standard mix of G1–G6; 1–7, incubation at 2, 5,10, 15, 30, 60 min and 18 h, respectively; and 8, substrate control.

Y171G, W275G, and W397F (with W275G having the most prominent signal). In G4 hydrolysis, an extra band corresponding toG5 was detected in the reaction with W168G, most likely due to be some tranglycosylation occurring concurrently with hydrolysis. Enhanced glycosylation was also recently found by Aronson et al. [35] in point mutation of the non-reducing end residue (Trp167 to Ala) for *S. marcescens* chitinase A.

With G5 and G6 substrates (Fig. 4C and D), the aromatic side chain mutants in general created more hydrolytic products than the wild-type enzyme. The breakdown of these substrates to G2 and G3 was best achieved by W275G, whereas the release of G1–G4 intermediates was preferred by W397F. On the other hand, W168G and Y171G seemed to behave similarly to the wild-type homologue, by releasing a small amount of G4 and greater amounts of G3 and G2 in the reactions with G5 substrate, while releasing comparable amounts of G4 and G2 in the reactions with G6 substrate.

The discrimination in substrate hydrolysis between wild-type and its mutants W275G and W397 was confirmed by time course experiments. Fig. 5A–C show the products formed by hydrolysis of G6 with the three variants at different times of reaction. Noticeably, both W275G and W397F hydrolyzed G6 much more efficiently than wild-type chitinase A. The reactions of W275G and W397F with G6 were already complete at 5 and 10 min, while substantial amounts of G6 were still present at these time points in the reaction mixture containing wild-type.

A further observation was that the three enzymes clearly adopted different modes of action on G6 substrate. This claim is supported by the fact that wild-type initially hydrolyzed G6 to G4 and G2. At the end of the reaction, G2 was produced as the major product (Fig. 5A). In contrast, W275G generated reaction intermediates of various lengths from G2 to G5 at initial times. Later, almost equal amounts of G2 and G3 were formed and this remained stable in course of reaction (Fig. 5B). On the other hand, W397F gave most distinct results by releasing a full range of G1–G5 products at early reaction times, eventually yielding G1 and G2 at the end (Fig. 5C).

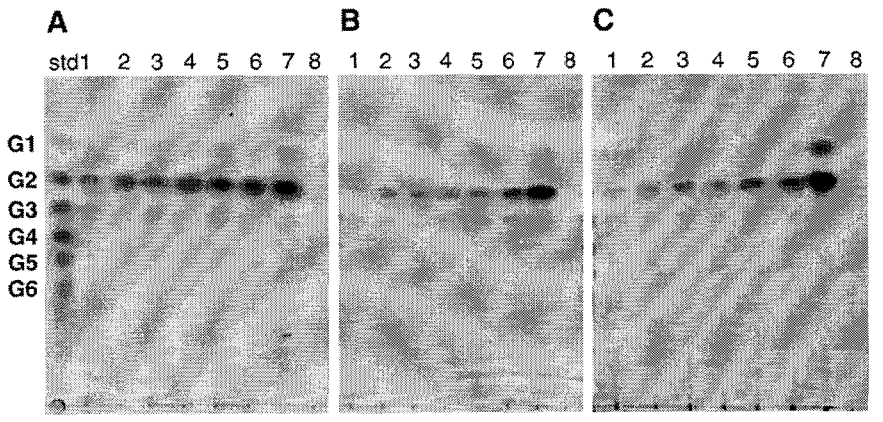

Fig. 6. Time-course of colloidal chitin hydrolysis by wild-type and mutants W275G and W397F. A reaction mixture (400 μl), containing 80 μg wild-type (A), W275G (B), or W397F (C) and 20 mg colloidal chitin in 0.1 M sodium acetate buffer, pH 5.0, was incubated at various times at 30 °C, and then analyzed by TLC using the same conditions as described for chitooligosaccharide hydrolysis. Lanes: std, standard mix of G1–G6; 1–7, incubation at 2, 5,10, 15, 30, 60 min and 18 h, respectively; and 8, substrate control.

The difference in cleavage patterns was not visible when the three enzymes were used to hydrolyze colloidal chitin (Fig. 6A–C). Over the first 60 min of incubation, the three enzymes essentially degraded chitin to G2 as the major product, with trace amounts of G3. Then, after 18 h, G2 and G1 were produced as the major end products, with some G3 also being present in the reaction of the W275G mutant.

The 3D-structure of *S. marcescens* chitinase A E315L mutant complexed with hexaNAG revealed that the oligosaccharide occupied subsites −4 to +2. An almost superimposition of the substrate binding clefts of *Vibrio* and *Serratia* enzymes (Fig. 2B) led to the assumption that oligosaccharide substrates would occupy the binding cleft of the *Vibrio* chitinase A in a similar manner as it was observed with the *Serratia* enzyme. Further investigation of the products released from penta- and hexaNAG hydrolyses by *S. marcescens* wild-type chitinase A demonstrated that both substrates only occupied subsites −2 to +2 with additional sugars extend beyond the substrate-binding cleft at the reducing end [22]. Such a four subsite binding mode seemed to also be the case for *B. circulans* chitinase A1 [27]. Even though the binding mode of the *Vibrio* enzyme cannot be specified at this point in time, the shift in the degradation patterns against chitooligomers upon particular point mutations gave indication that Trp275 and Trp397 are both important in the selective binding of soluble substrates.

A mutation of Trp397 to Phe results in an entire change in the cleavage patterns of the enzyme towards G6 and it can thus be assumed that Trp397 is involved in defining the primary binding sites for the incoming sugars so that the G2 and G4 will mainly be produced from the G6 substrate (Fig. 5A). Mutation of Trp397 to a less hydrophobic residue (Phe) seemed to loosen the binding affinity at this subsite. As a result, the incoming oligosaccharide had more freedom to assemble itself in the binding cleft, thus permitting various bonds to be exposed to the cleavage site (Fig. 5C). This finding is in a good agreement with the previous observations on *Serratia* and *Bacillus* chitinases [22,27]. Based on the −2 to +2 binding mode, Aronson et al. [22] suggested that the loss of binding affinity of the subsite +2 residue as a result of amino acid replacement (Trp396 to Ala) shifted the primary binding sites at least one position towards the non-reducing end.

Mutation of the +1 binding residue (Trp275) to Gly led to a major change in the hydrolysis of higher M_r oligosaccharides (as seen in Fig. 4B–D and Fig. 5B) by allowing the second and the third bonds of G6 from the non-reducing end (in the four subsite binding mode) to be equally accessed, confirming that Trp275 is involved in the specific binding of GlcNAc units around the cleavage site.

With colloidal chitin, no significant change in the cleavage patterns was seen as a result of the specific mutations of Trp275 and Trp397, which suggested that the two residues did not play the same role as in chitooligosaccharide degradation. According to "the feeding-sliding theory" suggested by Watanabe's group [23,27,34], a chitin polymer would enter the binding cleft unidirectionally from the non-reducing end rather than enter randomly like small substrates. Under these conditions, binding would be more influenced by a cluster of the surface-exposed amino acid residues that stretch along the *N*-terminal chitin binding domain through the substrate binding cleft than by particular residues.

Acknowledgements

This work was financially supported by Thailand Research Fund, The Thai Commission on Higher Education and the National Synchrotron Research Center (NSRC), Thailand. JS is a Senior Research Scholar of the Thailand Research Fund. CS was supported by a paid leave of absence from NSRC, Nakhon Ratchasima, Thailand. We would like to thank Dr. Chartchai Krittanai, Institute of Molecular Biology and Genetics, Mahidol University, Salaya, Nakhon Pathom, Thailand, for kindly providing the CD facility.

References

[1] C. Yu, A.M. Lee, B.L. Bassler, S. Roseman, Chitin utilization by marine bacteria. A physiological function for bacterial adhesion to immobilized carbohydrates, J. Biol. Chem. 266 (1991) 24260–24267.
[2] D.M. Rast, M. Horsch, R. Furter, G.W. Gooday, A complex chitinolytic system in exponentially growing mycelium of *Mucor rouxii*: properties and function, J. Gen. Microbiol. 137 (1991) 2797–2810.
[3] H. Merzendorfer, L. Zimoch, Chitin metabolism in insects: structure, function and regulation of chitin synthases and chitinases, J. Exp. Biol. 206 (2003) 4393–4412.
[4] A. Herrera-Estrella, I. Chet, Chitinases in biological control, EXS 87 (1999) 171–184.
[5] L.S. Melchers, M.H. Stuiver, Novel genes for disease-resistance breeding, Curr. Opin. Plant Biol. 3 (2000) 147–152.
[6] R.S. Patil, V.V. Ghormade, M.V. Deshpande, Chitinolytic enzymes: an exploration, Enzyme Microb. Technol. 26 (2000) 473–483.
[7] L.E. Donnelly, P.J. Barnes, Acidic mammalian chitinase—A potential target for asthma therapy, TRENDS Pharmacol. Sci. 25 (2004) 509–511.
[8] M. Wills-Karp, C.L. Karp, Chitin checking-novel insights into asthma, N. Engl. J. Med. 351 (2004) 1455–1457.
[9] W. Suginta, P.A. Robertson, B. Austin, S.C. Fry, L.A. Fothergill-Gilmore, Chitinases from *Vibrio*: activity screening and purification of chiA from *Vibrio carchariae*, J. Appl. Microbiol. 89 (2000) 76–84.
[10] W. Suginta, A. Vongsuwan, C. Songsiriritthigul, H. Prinz, P. Estibeiro, R.R. Duncan, J. Svasti, L.A. Fothergill-Gilmore, An endochitinase A from *Vibrio carchariae*: cloning, expression, mass and sequence analyses, and chitin hydrolysis, Arch. Biochem. Biophys. 424 (2004) 171–180.
[11] B. Henrissat, A. Bairoch, New families in the classification of glycosyl hydrolases based on amino acid sequence similarities, Biochem. J. 293 (1993) 781–788.
[12] A. Perrakis, I. Tews, Z. Dauter, A.B. Oppenheim, I. Chet, K.S. Wilson, C.E. Vorgias, Crystal structure of a bacterial chitinase at 2.3 Å resolution, Structure 2 (1994) 1169–1180.
[13] T. Hollis, A.F. Monzingo, K. Bortone, S. Ernst, R. Cox, J.D. Robertus, The X-ray structure of a chitinase from the pathogenic fungus *Coccidioides immitis*, Protein Sci. 9 (2000) 544–551.
[14] K. Suzuki, M. Taiyoji, N. Sugawara, N. Nikaidou, B. Henrissat, T. Watanabe, The third chitinase gene (chiC) of *Serratia marcescens* 2170 and the relationship of its product to other bacterial chitinases, Biochem. J. 343 (1999) 587–596.
[15] W. Suginta, A. Vongsuwan, C. Songsiriritthigul, J. Svasti, H. Prinz, Enzymatic properties of wild-type and active site mutants of chitinase A from *Vibrio carchariae*, as revealed by HPLC-MS, FEBS J. 272 (2005) 3376–3386.
[16] I. Tews, A.C. Terwisscha van Scheltinga, A. Perrakis, K.S. Wilson, B.W. Dijkstra, Substrate-assisted catalysis unifies two families of chitinolytic enzymes, J. Am. Chem. Soc. 119 (1997) 7954–7959.

[17] K.A. Brameld, W.A. Goddard III, Substrate distortion to a boat conformation at subsite −1 is critical in the mechanism of family 18 chitinases, J. Am. Chem. Soc. 120 (1998) 3571–3580.
[18] A.C. Terwisscha van Scheltinga, S. Armand, K.H. Kalk, A. Isogai, B. Henrissat, B.W. Dijkstra, Stereochemistry of chitin hydrolysis by a plant chitinase/lysozyme and X-ray structure of a complex with allosamidin: evidence for substrate assisted catalysis, Biochemistry 34 (1995) 15619–15623.
[19] D.M. van Aalten, D. Komander, B. Synstad, S. Gaseidnes, M.G. Peter, V.G. Eijsink, Structural insights into the catalytic mechanism of a family 18 exo-chitinase, Proc. Natl. Acad. Sci. U. S. A. 98 (2001) 8979–8984.
[20] C. Sasaki, A. Yokoyama, Y. Itoh, M. Hashimoto, T. Watanabe, T. Fukamizo, Comparative study of the reaction mechanism of family 18 chitinases from plants and microbes, J. Biochem. (Tokyo) 131 (2002) 557–564.
[21] T. Fukamizo, C. Sasaki, E. Schelp, K. Bortone, J.D. Robertus, Kinetic properties of chitinase-1 from the fungal pathogen *Coccidioides immitis*, Biochemistry 40 (2001) 2448–2454.
[22] N.N. Aronson Jr., B.A. Halloran, M.F. Alexyev, L. Amable, J.D. Madura, L. Pasupulati, C. Worth, P. Van Roey, Family 18 chitinase-oligosaccharide substrate interaction: subsite preference and anomer selectivity of *Serratia marcescens* chitinase A, Biochem. J. 376 (2003) 87–95.
[23] T. Watanabe, A. Ishibashi, Y. Ariga, M. Hashimoto, N. Nikaidou, J. Sugiyama, T. Matsumoto, T. Nonaka, Trp122 and Trp134 on the surface of the catalytic domain are essential for crystalline chitin hydrolysis by *Bacillus circulans* chitinase A1, FEBS Lett. 494 (2001) 74–78.
[24] T. Uchiyama, F. Katouno, N. Nikaidou, T. Nonaka, J. Sugiyama, T. Watanabe, Roles of the exposed aromatic residues in crystalline chitin hydrolysis by chitinase A from *Serratia marcescens* 2170, J. Biol. Chem. 276 (2001) 41343–41349.
[25] F. Katouno, M. Taguchi, K. Sakurai, T. Uchiyama, N. Nikaidou, T. Nonaka, J. Sugiyama, T. Watanabe, Importance of exposed aromatic residues in chitinase B from *Serratia marcescens* 2170 for crystalline chitin hydrolysis, J. Biochem. (Tokyo) 136 (2004) 163–168.
[26] Y. Itoh, J. Watanabe, H. Fukada, R. Mizuno, Y. Kezuka, T. Nonaka, T. Watanabe, Importance of Trp59 and Trp60 in chitin-binding, hydrolytic, and antifungal activities of *Streptomyces griseus* chitinase C, Appl. Microbiol. Biotechnol. 72 (2006) 1176–1184.
[27] T. Watanabe, Y. Ariga, U. Sato, T. Toratani, M. Hashimoto, N. Nikaidou, Y. Kezuka, T. Nonaka, J. Sugiyama, Aromatic residues within the substrate-binding cleft of *Bacillus circulans* chitinase A1 are essential for hydrolysis of crystalline chitin, Biochem. J. 376 (2003) 237–244.
[28] Collaborative Computational Project, Number 4, The CCP4 suit: programs for protein crystallography, Acta Cryst. D50 (1994) 760–763.
[29] U.K. Laemmli, Cleavage of structural proteins during the assembly of the head of bacteriophage T4, Nature 227 (1970) 680–685.
[30] M.M. Bradford, A rapid and sensitive method for the quantitation of microgram quantities of protein utilizing the principle of protein-dye binding, Anal. Biochem. 72 (1976) 248–254.
[31] A. Bruce, U. Srinivasan, H.J. Staines, T.L. Highley, Chitinase and laminarinase production in liquid culture by *Trichoderma* spp. and their role in biocontrol of wood decay fungi, Int. Biodeterior. Biodegrad. 35 (1995) 337–353.
[32] S.C. Hsu, J.L. Lockwood, Powdered chitin agar as a selective medium for enumeration of actinomycetes in water and soil, Appl. Microbiol. 29 (1975) 422–426.
[33] T. Tanaka, S. Fujiwara, S. Nishikori, T. Fukui, M. Takagi, T. Imanaka, A unique chitinase with dual active sites and triple substrate binding sites from the hyperthermophilic Archaeon *Pyrococcus kodakaraensis* KOD1, Appl. Environ. Microbiol. 15 (1999) 5338–5344.
[34] T. Imai, T. Watanabe, T. Yui, J. Sugiyama, Directional degradation of beta-chitin by chitinase A1 revealed by a novel reducing end labelling technique, FEBS Lett. 510 (2002) 201–205.
[35] N.N. Aronson Jr., B.A. Halloran, M.F. Alexeyev, X.E. Zhou, Y. Wang, E.J. Meehan, L. Chen, Mutation of a conserved tryptophan in the chitin-binding cleft of *Serratia marcescens* chitinase A enhances transglycosylation, Biosci. Biotechnol. Biochem. 70 (2006) 243–251.